HHS Public Access

Author manuscript

Anal Chem. Author manuscript; available in PMC 2024 May 23.

Published in final edited form as:

Anal Chem. 2024 May 14; 96(19): 7506–7515. doi:10.1021/acs.analchem.4c00182.

Probing Protein Structural Changes in Alzheimer's Disease via Quantitative Cross-linking Mass Spectrometry

Zexin Zhu[1,#], **Xiaofang Zhong**[1,2,#], **Bin Wang**[1,#], **Haiyan Lu**[1], **Lingjun Li**[1,3,4,5,*]

[1]School of Pharmacy, University of Wisconsin-Madison, Madison, WI, 53705, United States

[2]Department of Cellular and Molecular Pharmacology, University of California-San Francisco, San Francisco, CA 94158, USA

[3]Department of Chemistry, University of Wisconsin-Madison, Madison, WI, 53706, USA

[4]Lachman Institute for Pharmaceutical Development, School of Pharmacy, University of Wisconsin-Madison, Madison, WI 53705, USA

[5]Wisconsin Center for NanoBioSystems, School of Pharmacy, University of Wisconsin-Madison, Madison, WI 53705, USA.

Abstract

Alzheimer's disease (AD) is a progressive neurological disorder, featured by abnormal protein aggregation in the brain, including the pathological hallmarks of amyloid plaques and hyperphosphorylated tau. Despite extensive research efforts, understanding the molecular intricacies driving AD development remains a formidable challenge. This study focuses on identifying key protein conformational changes associated with the progression in AD. To achieve this, we employed quantitative crosslinking mass spectrometry (XL-MS) to elucidate conformational changes in the protein networks in cerebrospinal fluid (CSF). By using isotopically labeled crosslinkers BS^3d_0 and BS^3d_4, we reveal a dynamic shift in protein interaction networks during AD progression. Our comprehensive analysis highlights distinct alterations in protein-protein interactions within Mild Cognitive Impairment (MCI) states. This study accentuates the potential of crosslinked peptides as indicators of AD-related conformational changes, including previously unreported site-specific binding between alpha-1-antitrypsin (A1AT) and Complement Component 3 (CO3). Furthermore, this work enables detailed structural characterization of Apolipoprotein E (ApoE) and reveals modifications within its helical domains, suggesting their involvement in MCI pathogenesis. The quantitative approach provides insights into site-specific interactions and changes in the abundance of crosslinked peptides, offering an improved understanding of the intricate protein-protein interactions underlying AD progression. These findings lay a foundation for the development of potential diagnostic or therapeutic strategies aimed at mitigating the negative impact of AD.

Graphical Abstract

*Corresponding author: Fax: +1 (608) 262-5345, lingjun.li@wisc.edu.
#These authors contributed equally to this work.

Supporting information

Additional information as noted in text. This material is available free of charge via the Internet at http://pubs.acs.org.

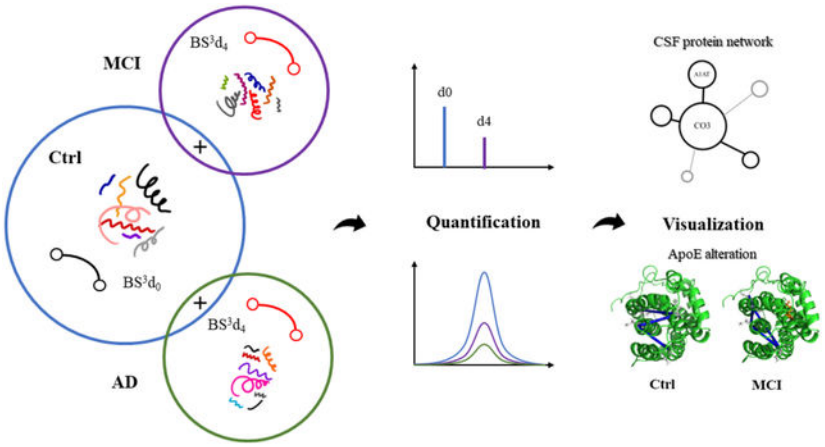

Keywords

crosslinking mass spectrometry (XL-MS); quantitative proteomics; Alzheimer's disease; protein-protein interaction; conformational changes; neurodegenerative disease

Introduction

As one of the most prominent public health concerns, Alzheimer's disease (AD) has affected more than 6.7 million people in the US and is ranked as the fifth leading cause of death among those aged 65 or older[1]. Rooted in synaptic homeostasis disruption and intricate signaling pathway dysfunction, AD is marked by progressive cognitive impairment. During the course of AD progression, mild cognitive impairment (MCI) has been reported as an intermediate state and about 15% of patients are diagnosed as MCI patients before AD dementia. The MCI stage manifests varied cognitive deficits, including memory loss, attention deficits, and language impairment[2]. Although the major pathological theory of amyloid beta (Aβ) fibrillation and plaque formation have been extensively documented, recent research suggests that Aβ modification only involves certain heterogeneous pathways and therapeutic advancements based on Aβ have been frustratingly slow[3–5]. In parallel, Tau phosphorylation has been implicated in the formation of the neurofibrillary tangles (NFTs) formation, which contributes to the collapse of cytoarchitecture and subsequent neuronal degradation[6]. Despite the significant attention to Tau topology, clinical progress is hampered by concerns regarding efficacy and toxicity[7]. Thus, the identification of alternative biomarker candidates is imperative for precision AD therapeutics. In particular, the transition from MCI to full-blown AD represents a critical juncture in AD's trajectory, underscoring the urgent need for effective interventions during this intermediate phase.

Mass spectrometry (MS) has emerged as an exceptional tool for the identification of protein structures and the characterization of conformational networks in recent decades. Among the various branches of MS techniques, crosslinking mass spectrometry (XL-MS) is an emerging approach that provides insights into structural dynamics[8, 9]. It involves the use of a chemical reagent known as crosslinker, which forms new covalent bonds between specific amino acids. In general, crosslinkers consist of two reactive groups at the ends and a spacer

arm bridging them. Each crosslinker has a defined distance threshold, within which only residues that are spatially proximate can be crosslinked[10]. When the data of crosslinked sites are obtained through MS acquisition, the compilation of the result can reveal structural information about the protein complex or the topology of the protein network. The primary advantage of XL-MS is the crosslinked peptides are stable and can withstand a wide range of buffer conditions[11]. Therefore, the application of the XL-MS is versatile, ranging from conformational changes in single protein or complex to *in vivo* systematic study of protein-protein network[12]. In addition, quantitative XL-MS (QXL-MS) enables direct comparison of crosslinking in different states of flexible regions. The incorporation of isotopically labeled crosslinkers provide extra separation between targeted peaks and allow for the detection of conformational changes through abundance quantification[13]. Numerous successful studies have demonstrated the elucidation of protein interactomes via chemical crosslinking strategy[14–16].

This study seeks to identify potential protein factors that can serve as indicators of AD prognosis. Hereby, we investigate the conformational changes in protein networks during AD development using human cerebrospinal fluids (CSF) samples. Leveraging the quantitative XL-MS (QXL-MS), our research provides critical insights into the dynamic shifts in protein-protein interaction networks as AD progresses. By visualizing the data, we aim to shed light on alternative biomarker candidates, thereby providing a hypothetical framework that elucidates the site-specific binding within the intricate protein structures. These new findings will facilitate the development of more precise diagnostic tools and therapeutic strategies for AD and related dementia.

Experimental Section

AD CSF Samples and Chemical Reagents

All human subjects involved in this study have received approval from the University of Wisconsin Institutional Review Board. The study comprised of 48 participants from the Wisconsin Alzheimer's Disease Research Center (ADRC), who were individually selected from healthy controls, MCI, and AD groups (Supplemental Table S1).

CSF Protein Crosslinking

The detailed workflow of the overall processing experiments is shown in Figure 1. The protein concentration of the CSF samples was determined via BCA protein assay kit from Thermo (Pittsburgh, PA). Approximately 100 μg protein of from each sample was used for the crosslinking incubation. The BS3 (bis[sulfosuccinimidyl] suberate) crosslinkers were dissolved in water to obtain a stock concentration of 50 mM and the final reaction concentration was 1 mM. The control sample was incubated with BS^3d_0, whereas the MCI or AD sample was incubated with BS^3d_4 (deuterium-labeled isotopomer) in 20 mM HEPES buffer for 1 hour (Figure S1)[17, 18]. The crosslinking reaction was terminated with 20 mM Tris buffer for 20 min. BS^3d_0 and BS^3d_4 cross-linked samples were mixed with a 1:1 ratio and subjected to Albumin Depletion Kit purchased from Pierce (Waltham, MA) to remove albumin.

Tryptic Proteolysis

The samples were digested with a filter-aided sample preparation (FASP) procedure[19]. In brief, the crosslinked samples were washed three times with 8 M urea using a 30 kDa molecular weight cutoff filter (Millipore). The samples were reduced with 20 mM dithiothreitol (DTT) for 45 minutes, alkylated with 20 mM iodoacetamide (IAA) in the dark for 45 minutes, and digested with trypsin (enzyme: protein = 1: 40) from Promega (Madison, WI) overnight at 37°C. The digestion process is quenched with 10% Trifluoroacetic Acid (TFA) to reach a condition pH < 3. For in-solution digestion, the crosslinked protein sample was mixed with 8M urea at a 1:2 (vol/vol) ratio. For enhanced FASP (eFASP), the samples were washed with 8M urea in 0.1% deoxycholic acid (DCA) from Sigma-Aldrich (St. Louis, MO)[20, 21]. All the other following steps were the same as described in FASP. The peptides were subsequently desalted through a Bond Elut OMIX C18 pipet tips with 80% ACN and 0.1% Formic Acid (FA) elution. The eluted sample was dried down in SpeedVac Vacuum Concentrator before MS acquisition.

LC-MS/MS analysis

Samples were run through Thermo Fusion Lumos Orbitrap Tribrid mass spectrometer. The sample was redissolved in 97% Optima water, 3% ACN, and 0.1% FA, and loaded to the Dionex UltiMate 3000 UPLC system. The separation was done via a homemade microcapillary column (75-μm inner diameter) packed with 18 cm of Bridged Ethylene Hybrid C18 particles (1.7 μm, 130 Å, Waters). LC separation is achieved via 100 minutes of gradient elution of 3% mobile phase B (pure ACN with 0.1% FA) to 95%, with a flow rate of 300 nL/min. The acquisition method is set under high-collisional dissociation (HCD) with a resolving power of 120k, scanning range from 400–1600 *m/z*, and maximum injection time of 50 ms. The data dependent mode was set to 3 seconds between master scans with a normalized collision energy of 30. MS2 acquisition was performed with an isolation window of 2 Da, resolving power of 30k, and standard AGC target.

Quantitative Structural Analysis and Visualization

Crosslink signals in the raw files were searched via Xisearch (version 1.7.6.7) against the UniProt *Homo sapiens* reviewed database. Both BS3 light (BS^3d_0) and BS3 heavy (BS^3d_4) were selected for searching[13, 22, 23]. For the identification parameters, trypsin was selected as enzyme digestion, and maximum 3 of miscleavage was chosen. Precursor tolerance is 20 ppm and False Discovery Rate (FDR) is controlled at < 5% at PSM level. To increase the efficiency of the algorithm running and filter the low-scored crosslinks interference, we only selected top 20 proteins from human proteome FASTA file that has most available crosslinks (Table S2). The quantitation work was performed through Skyline (version 22.2.0) with the library file in.ssl version imported from Xisearch[24]. All decoy crosslinks are excluded prior to the Skyline analysis. The dot product value (dotp) was set to above 0.9 and the peak area comparison of each target in the library list was manually checked to ensure more than 50% of the replicate in each set reached the dotp line. One set of BS^3d_0 (Ctrl group) and both sets of BS^3d_4 (MCI and AD) group were selected for the subsequent analysis and Skyline library construction. The peptide set remained consistent with the previous crosslinking search, while in the transition setting, the precursor charges ranged

from 3 to 7. The fold change values of AD:Ctrl and MCI:Ctrl were calculated based on the quantitation result output via Skyline, and the p-value was derived from the analysis of the 16 replicates. The threshold for the p-value is determined over 0.05 and the fold change is equal to 1. The volcano plot is depicted to highlight the upregulation and downregulation of the crosslinked peptides. To visualize our data, including bar charts, bubble charts, and volcano plots, we used HiPlot websites and Python programming[25]. The .mgf file converted from raw data, FASTA file, and .mzML file from xiSearch was uploaded to xiView for 2D protein-protein network mapping[26]. For the 3D model for the protein structures, we employed PyMOL and ChimeraX 1.3[25, 27, 28]. Additionally, for Gene Ontology analysis, the DAVID bioinformatics resources were applied with highlight of biological process, cellular component and molecular function[29].

Results and Discussion

Crosslinking MS reveals conformational variation within CSF protein networks during AD progression

Prior to the investigation of all human CSF samples, we compared the in-solution, eFASP, and FASP digestion methods to assess their compatibility with crosslinking proteins. Using BS^3d_0 labeled CSF from one control sample, the numbers of crosslinked spectral matches being identified were 126, 218, and 254, and the numbers of peptides were 80, 85, 109 in in-solution, eFASP, and FASP digestions methods, respectively. The performance of FASP and eFASP were comparable, but both outperformed in-solution digestion (Figure S1). Consequently, we opted to employ FASP for subsequent sample preparation.

Furthermore, the presence of albumin in substantial quantities within the CSF samples posed a significant challenge. Albumin is the most abundant protein in human plasma because of its high concentration and large molecular weight[30, 31]. It is rich in Lysine residues, which are specifically targeted by our selected crosslinkers. Both BS^3d_0 and BS^3d_4 are homobifunctional crosslinkers with spacer arms of the same length (11.4 Å) and sulfo-NHS reactive groups on both ends, which attach to the primary amine groups on Lysine residues and the N-termini of peptides. We observed that over 40% of the crosslinks were type-1 intralinks within the albumin itself. This raised concerns that without the removal of albumin, the presence of albumin-derived crosslinking peptides could obscure the detection of crosslinks involving other CSF proteins. Herein, we subjected the CSF samples through albumin depletion resin to generate a more comprehensive view of interlinks among all potential protein biomarkers. The number of unique interlink matchups between different proteins after albumin depletion has been doubled in comparison to the same sample replicate without albumin depletion (Figure S3).

The analysis of our data revealed a noteworthy pattern: a significant decrease in the overall number of crosslinked spectral matches and unique crosslinked peptides from the control (Ctrl) group to MCI and further to the AD condition (Figure 2a). In the summary of the overall 16 sets of sample replicates, the Ctrl group exhibited almost double the number of discovered crosslinked spectral matches and unique crosslinked peptides compared to the AD group. Notably, the substantial proportion of observations within individual sets underscores the complexity of the conditions under investigation. This phenomenon was

most pronounced in the Ctrl condition, where 66.5% of the XL matches were unique, while in the AD and MCI conditions, less than 50% of the matches were retained (Figure 2b). In terms of intersectional crosslinking in overlapped area, the greatest number of interlinks shared between Ctrl and MCI groups was observed, whereas the Ctrl-AD set exhibited the fewest preserved crosslinks. These findings highlight the significant alterations in crosslinking patterns between healthy controls and the AD condition, with MCI serving as an intermediate stage preserving a substantial number of interlinks from both conditions.

The identified crosslinked proteins were used for protein-protein interaction (PPI) analysis, which includes majority of plasma proteins: apolipoprotein (APOA1 and APOE), transferrin (TRFE), alpha-1-antitrypsin (A1AT), alpha-2-microglobulin (A2MG), complement components (CO3, CO5, CFAB), alpha-1-antichymotrypsin (AACT), antithrombin (ANT3), vitamin-D binding protein (VTDB) (Figure 2c). We identified several representative biomarkers that are pertinent to Alzheimer's disease (AD) development. One such biomarker is Clusterin (CLUS), whose conformational changes in AD have been previously reported in our earlier research[32]. To assess the reliability of our crosslinking map, we compared the crosslinking PPI mapping with the previously validated colocalization or co-expression traits using these successfully identified crosslinked proteins from the STRING database[33]. We manually input these crosslinked proteins and compared their PPI interaction shape with our xiView output (Figure 2d–f). As a result, more than 85% of the crosslinks and PPI have been previously confirmed by other studies or publications[34–36]. For instance, the direct interaction between transferrin and antithrombin has been verified in the previous publication via surface plasmon resonance (SPR) analysis, whereas a significant number of TRFE-ANT3 interlinks has been reported in both Ctrl and MCI group in our experiment[35]. This validation suggests that our crosslinking strategy delineates a genuine protein-protein interaction network in the selected CSF samples. From the visualization of the networks, xiView mapping also indicates that most of the PPI are centered around TRFE and complement component 3 (CO3) across all three different cases. The cluster of the interlinking between different proteins on these two anchors is even greater in MCI but in the AD group this TRFE-centered correlation is restrained because of fewer crosslinking matches and PPI. These findings strongly suggest that the protein interaction network is greatly affected during AD progression.

Quantitative analysis highlights distinctive site-specific protein structural changes as potential biomarkers for AD

While numerous publications have reported the CSF proteomic and corresponding pathological alterations during AD progression, the structural information within the protein complex or docking domains remains elusive[37–39]. Hence, our quantitative XL-MS workflow, executed through Skyline, presents a novel strategy highlighting site-specific interaction between CSF biomarkers. The crosslinking data were processed according to the methodology outlined in the Experimental Section. The volcano plot serves as a rapid means of identifying crosslink abundance alterations across multiple sample replicates (Figure 3a–b). In the comparison between AD and Ctrl, nine crosslinks exhibited higher abundance in the AD group, while seven crosslinks were retained mostly in Ctrl group. Notably, the numbers shifted to 27 up- and 12 down-regulated crosslinks in the MCI-Ctrl comparison,

highlighting the dynamic conformational changes in protein-protein interactions during disease progression from MCI to AD.

Among these significantly upregulated or downregulated crosslinks, many involve interlinks between diverse biomarkers, but the proportion of type 2 interlinks between different proteins is less than 40% of the overall crosslinks. Particularly noteworthy are the crosslink pairs that relate to CO3 and A1AT. In recent years, extensive research has focused on the interaction between CO3 and A1AT. Dysregulated complement activation has been demonstrated to have a strong impact on tau pathology and neurological damage[40–43]. A1AT may form covalent-binding aggregates along with VDTB and induce formation of the neutrophil[44, 45]. Meanwhile, this relative VDTB interaction is also successfully identified in the crosslinking network (Figure 2d–e). However, the nature of the aggregates between CO3 and A1AT remains poorly understood. In 2021, the structural insights into the complement complex were validated through *in vivo* crosslinking, supported by X-ray crystallography[46]. Our crosslink result proposes a hypothetical model detailing the site-specific binding between A1AT and CO3 (Table S3). Quantitative findings reveal a high degree of activity for A1AT at K246 in crosslinking with CO3 Lysine residues. This crosslink accounts for approximately 70% of the unique crosslinking matches, however, the composition of its crosslinking is very different from each other (Table S4). The crosslinks between A1AT K246 and CO3 K685 were identified in both Ctrl and MCI groups, but the intensity in MCI was significantly lower than that in Ctrl (Figure 3c). Conversely, the A1AT K246 – CO3 K428 crosslink demonstrated a preference towards MCI and AD cases, with the abundance in AD almost twice as high as in MCI. This indicates a dynamic change in the interaction between these two proteins during the progression of AD (Figure 3d). It is noteworthy that these two crosslinked residues are located on two different chains, albeit in close proximity to each other in protein crystallography: K428 is on the conserved macroglobulin domain and K685 is on the anaphylatoxin (ANA) domain, which is the key of C3a fragment during cleavage[47] (Figure 3e). These findings further support the stepwise alteration in activation and subsequent signaling cascades throughout MCI and AD development.

To delve deeper into the functions that these crosslinked proteins are involved, we conducted both Gene Oncology Enrichment and Kyoto Encyclopedia of Genes and Genomes (KEGG) pathway analyses (Figure 4a, 4b). These analyses revealed associations with serine-type endopeptidase inhibitor activity, the complement and coagulation cascade, and AD-specific terms, including the regulation of beta-amyloid clearance, tau protein binding, and the regulation of platelet or fibril formation. In summary, our findings demonstrate the involvement of protein biomarkers that are particularly pertinent to the progression of AD.

Intralinks reveals potential structural alteration in ApoE during MCI development

Apolipoprotein E (ApoE) plays a pivotal role in AD as a risk factor for neuropathology and pathogenesis of AD[48]. Within the CSF, ApoE serves as a critical regulator in multiple signaling pathways and the maintenance of the central nervous system (CNS)[49]. It has three main alleles E2, E3 and E4, which differed primarily at positions 112 and 158 in the amino acid sequence[50]. These structural variations between isoforms, especially in the major helix region on the C-terminal domain, are known to influence overall

protein stabilization and functionality in the AD[50–52]. Consequently, our focus centers on identifying and examining variations in crosslinks within ApoE during the development of MCI. Intralinks analysis provides insights indicating that specific interactions within the helix structures are retained in both conditions: ApoE K90-K113 and ApoE K251-K260. The K251-K260 interaction occurs within the C-terminal regions, which is implicated in oligomer formation and amyloid beta (Aβ) binding[37]. Our quantitative findings highlight the consistency in the abundance of this linkage across multiple sample sets for comparison (Figure 5a), suggesting the potential pathological binding between ApoE and heparan sulfate (HS) remains unaffected under MCI stage[53]. The underlying hypothesis that HS-assisted accumulation and induction with tau protein is not supported[54, 55]. Concurrently, differences in crosslink patterns between the control and MCI conditions become evident. In the control group, K175 exhibits robust crosslinking, seen in K113-K175 and K175-K260 interactions across multiple replicates. In contrast, these crosslinks are not discernible in the MCI condition through xiSearch, due to a pronounced decrease in abundance (Figure 5b). Instead, alternate crosslinking sites remain active in the control group, including interactions like K90-K260 and K113-K260, detected across various samples. These observations collectively suggest a substantial structural transformation in ApoE during the course of MCI progression. Lysine 175, located within helix 4, a highly charged domain containing the low-density lipoprotein receptor (LDLR) binding site, emerges as a focal point of this conformational shift[51]. Our intralink analysis reveals that the conformational change at Lysine 175 may disrupt the interaction with helix 4 in ApoE (Figure 5c–d). This disruption could potentially contribute to abnormal binding processes, ultimately leading to amyloid deposition[56]. The alteration in the conformation of this region could also impact receptor interactions, potentially affecting cellular uptake and clearance mechanisms. Future work will be directed to substantiate our hypothesis using computational platforms such as HADDOCK[57]. Additionally, we aim to extract the ApoE protein for more precise 3D remodeling during AD progression.

Conclusion

This study employs XL-MS to investigate the intricate structural changes within CSF protein networks during the progression of MCI and AD. The comprehensive analysis reveals a dynamic shift in protein interaction networks as the pathological condition advances. The alterations in protein-protein interactions provide crucial insights into the proteomic changes associated with AD development. Furthermore, our investigation delves into the structural alterations of key biomarkers, with a particular focus on the interaction between A1AT and CO3, as well as the conformational changes within ApoE, shedding light on their potential involvement in AD pathogenesis. The observed site-specific interactions and changes in crosslink abundance offer a detailed understanding of the molecular intricacies underlying AD progression. The insights gained from this research not only open new avenues for the study of AD, but also provide potential directions for advancing our knowledge of neurodegenerative diseases and developing effective therapeutic strategies.

Supplementary Material

Refer to Web version on PubMed Central for supplementary material.

Acknowledgements

This research was supported, in part, by the National Institutes of Health Grants R21AG065728, R01AG052324, R01AG078794, and R01DK071801. Some of the mass spectrometers were acquired using NIH shared instrument grants S10 OD028473, S10 RR029531, and S10 OD025084. H.L. wishes to thank the funding support for a Postdoctoral Career Development Award provided by the American Society for Mass Spectrometry. L.L. acknowledges a Vilas Distinguished Achievement Professorship and Charles Melbourne Johnson Distinguished Chair Professorship with funding provided by the Wisconsin Alumni Research Foundation and University of Wisconsin-Madison, School of Pharmacy.

Data Availability

The mass spectrometry raw data, peak list and the mzid files has been uploaded through Mass Spectrometry Interactive Virtual Environment (MassIVE) and deposited in ProteomeXchange. The accession number is MSV000094259 for MassIVE and PXD050457 for ProteomeXchange.

References

1. 2023 Alzheimer's disease facts and figures. Alzheimers Dement 2023.
2. Farias ST; Mungas D; Reed BR; Harvey D; DeCarli C, Progression of mild cognitive impairment to dementia in clinic- vs community-based cohorts. Arch Neurol 2009, 66 (9), 1151–7. [PubMed: 19752306]
3. Mullane K; Williams M, Alzheimer's disease (AD) therapeutics - 1: Repeated clinical failures continue to question the amyloid hypothesis of AD and the current understanding of AD causality. Biochem Pharmacol 2018, 158, 359–375. [PubMed: 30273553]
4. Long JM; Holtzman DM, Alzheimer Disease: An Update on Pathobiology and Treatment Strategies. Cell 2019, 179 (2), 312–339. [PubMed: 31564456]
5. Chiti F; Dobson CM, Protein misfolding, functional amyloid, and human disease. Annu Rev Biochem 2006, 75, 333–66. [PubMed: 16756495]
6. Xia Y; Prokop S; Giasson BI, "Don't Phos Over Tau": recent developments in clinical biomarkers and therapies targeting tau phosphorylation in Alzheimer's disease and other tauopathies. Mol Neurodegener 2021, 16 (1), 37. [PubMed: 34090488]
7. Congdon EE; Sigurdsson EM, Tau-targeting therapies for Alzheimer disease. Nat Rev Neurol 2018, 14 (7), 399–415. [PubMed: 29895964]
8. Yu C; Huang L, Cross-Linking Mass Spectrometry: An Emerging Technology for Interactomics and Structural Biology. Anal Chem 2018, 90 (1), 144–165. [PubMed: 29160693]
9. Liu F; Heck AJ, Interrogating the architecture of protein assemblies and protein interaction networks by cross-linking mass spectrometry. Curr Opin Struct Biol 2015, 35, 100–8. [PubMed: 26615471]
10. Piersimoni L; Kastritis PL; Arlt C; Sinz A, Cross-Linking Mass Spectrometry for Investigating Protein Conformations and Protein-Protein Interactions horizontal line A Method for All Seasons. Chem Rev 2022, 122 (8), 7500–7531. [PubMed: 34797068]
11. O'Reilly FJ; Rappsilber J, Cross-linking mass spectrometry: methods and applications in structural, molecular and systems biology. Nat Struct Mol Biol 2018, 25 (11), 1000–1008. [PubMed: 30374081]
12. Matzinger M; Mechtler K, Cleavable Cross-Linkers and Mass Spectrometry for the Ultimate Task of Profiling Protein-Protein Interaction Networks in Vivo. J Proteome Res 2021, 20 (1), 78–93. [PubMed: 33151691]
13. Chen ZA; Rappsilber J, Quantitative cross-linking/mass spectrometry to elucidate structural changes in proteins and their complexes. Nat Protoc 2019, 14 (1), 171–201. [PubMed: 30559374]
14. Gomez-Ramirez J; Wu J, Network-based biomarkers in Alzheimer's disease: review and future directions. Front Aging Neurosci 2014, 6, 12. [PubMed: 24550828]
15. Rey M; Dhenin J; Kong Y; Nouchikian L; Filella I; Duchateau M; Dupre M; Pellarin R; Dumenil G; Chamot-Rooke J, Advanced In Vivo Cross-Linking Mass Spectrometry Platform to

Characterize Proteome-Wide Protein Interactions. Anal Chem 2021, 93 (9), 4166–4174. [PubMed: 33617236]

16. Wheat A; Yu C; Wang X; Burke AM; Chemmama IE; Kaake RM; Baker P; Rychnovsky SD; Yang J; Huang L, Protein interaction landscapes revealed by advanced in vivo cross-linking-mass spectrometry. Proc Natl Acad Sci U S A 2021, 118 (32), No. e2023360118.
17. Muller DR; Schindler P; Towbin H; Wirth U; Voshol H; Hoving S; Steinmetz MO, Isotope-tagged cross-linking reagents. A new tool in mass spectrometric protein interaction analysis. Anal Chem 2001, 73 (9), 1927–34. [PubMed: 11354472]
18. Sinz A, Chemical cross-linking and mass spectrometry for mapping three-dimensional structures of proteins and protein complexes. J Mass Spectrom 2003, 38 (12), 1225–37. [PubMed: 14696200]
19. Wisniewski JR; Zougman A; Nagaraj N; Mann M, Universal sample preparation method for proteome analysis. Nat Methods 2009, 6 (5), 359–62. [PubMed: 19377485]
20. Erde J; Loo RR; Loo JA, Improving Proteome Coverage and Sample Recovery with Enhanced FASP (eFASP) for Quantitative Proteomic Experiments. Methods Mol Biol 2017, 1550, 11–18. [PubMed: 28188519]
21. Lu L; Millikin RJ; Solntsev SK; Rolfs Z; Scalf M; Shortreed MR; Smith LM, Identification of MS-Cleavable and Noncleavable Chemically Cross-Linked Peptides with MetaMorpheus. J Proteome Res 2018, 17 (7), 2370–2376. [PubMed: 29793340]
22. Mendes ML; Fischer L; Chen ZA; Barbon M; O'Reilly FJ; Giese SH; Bohlke-Schneider M; Belsom A; Dau T; Combe CW; Graham M; Eisele MR; Baumeister W; Speck C; Rappsilber J, An integrated workflow for crosslinking mass spectrometry. Mol Syst Biol 2019, 15 (9), e8994. [PubMed: 31556486]
23. UniProt C, UniProt: the Universal Protein Knowledgebase in 2023. Nucleic Acids Res 2023, 51 (D1), D523–D531. [PubMed: 36408920]
24. MacLean B; Tomazela DM; Shulman N; Chambers M; Finney GL; Frewen B; Kern R; Tabb DL; Liebler DC; MacCoss MJ, Skyline: an open source document editor for creating and analyzing targeted proteomics experiments. Bioinformatics 2010, 26 (7), 966–8. [PubMed: 20147306]
25. Li J; Miao B; Wang S; Dong W; Xu H; Si C; Wang W; Duan S; Lou J; Bao Z; Zeng H; Yang Z; Cheng W; Zhao F; Zeng J; Liu XS; Wu R; Shen Y; Chen Z; Chen S; Wang M; Hiplot C, Hiplot: a comprehensive and easy-to-use web service for boosting publication-ready biomedical data visualization. Brief Bioinform 2022, 23 (4), No. bbac261.
26. Combe CW; Fischer L; Rappsilber J, xiNET: cross-link network maps with residue resolution. Mol Cell Proteomics 2015, 14 (4), 1137–47. [PubMed: 25648531]
27. Goddard TD; Huang CC; Meng EC; Pettersen EF; Couch GS; Morris JH; Ferrin TE, UCSF ChimeraX: Meeting modern challenges in visualization and analysis. Protein Sci 2018, 27 (1), 14–25. [PubMed: 28710774]
28. Pettersen EF; Goddard TD; Huang CC; Meng EC; Couch GS; Croll TI; Morris JH; Ferrin TE, UCSF ChimeraX: Structure visualization for researchers, educators, and developers. Protein Sci 2021, 30 (1), 70–82. [PubMed: 32881101]
29. Sherman BT; Hao M; Qiu J; Jiao X; Baseler MW; Lane HC; Imamichi T; Chang W, DAVID: a web server for functional enrichment analysis and functional annotation of gene lists (2021 update). Nucleic Acids Res 2022, 50 (W1), W216–W221. [PubMed: 35325185]
30. LeVine SM, Albumin and multiple sclerosis. BMC Neurol 2016, 16, 47. [PubMed: 27067000]
31. Menendez-Gonzalez M; Gasparovic C, Albumin Exchange in Alzheimer's Disease: Might CSF Be an Alternative Route to Plasma? Front Neurol 2019, 10, 1036. [PubMed: 31681137]
32. Foster EM; Dangla-Valls A; Lovestone S; Ribe EM; Buckley NJ, Clusterin in Alzheimer's Disease: Mechanisms, Genetics, and Lessons From Other Pathologies. Front Neurosci 2019, 13, 164. [PubMed: 30872998]
33. Szklarczyk D; Kirsch R; Koutrouli M; Nastou K; Mehryary F; Hachilif R; Gable AL; Fang T; Doncheva NT; Pyysalo S; Bork P; Jensen LJ; von Mering C, The STRING database in 2023: protein-protein association networks and functional enrichment analyses for any sequenced genome of interest. Nucleic Acids Res 2023, 51 (D1), D638–D646. [PubMed: 36370105]
34. Shah A; Kishore U; Shastri A, Complement System in Alzheimer's Disease. Int J Mol Sci 2021, 22 (24), 13467. [PubMed: 34948264]

35. Tang X; Zhang Z; Fang M; Han Y; Wang G; Wang S; Xue M; Li Y; Zhang L; Wu J; Yang B; Mwangi J; Lu Q; Du X; Lai R, Transferrin plays a central role in coagulation balance by interacting with clotting factors. Cell Res 2020, 30 (2), 119–132. [PubMed: 31811276]
36. Varma VR; Varma S; An Y; Hohman TJ; Seddighi S; Casanova R; Beri A; Dammer EB; Seyfried NT; Pletnikova O; Moghekar A; Wilson MR; Lah JJ; O'Brien RJ; Levey AI; Troncoso JC; Albert MS; Thambisetty M, Alpha-2 macroglobulin in Alzheimer's disease: a marker of neuronal injury through the RCAN1 pathway. Mol Psychiatry 2017, 22 (1), 13–23. [PubMed: 27872486]
37. Wang B; Zhong X; Fields L; Lu H; Zhu Z; Li L, Structural Proteomic Profiling of Cerebrospinal Fluids to Reveal Novel Conformational Biomarkers for Alzheimer's Disease. J Am Soc Mass Spectrom 2023, 34 (3), 459–471. [PubMed: 36745855]
38. Maccarrone G; Milfay D; Birg I; Rosenhagen M; Holsboer F; Grimm R; Bailey J; Zolotarjova N; Turck CW, Mining the human cerebrospinal fluid proteome by immunodepletion and shotgun mass spectrometry. Electrophoresis 2004, 25 (14), 2402–12. [PubMed: 15274023]
39. Wenner BR; Lovell MA; Lynn BC, Proteomic analysis of human ventricular cerebrospinal fluid from neurologically normal, elderly subjects using two-dimensional LC-MS/MS. J Proteome Res 2004, 3 (1), 97–103. [PubMed: 14998169]
40. O'Brien ME; Fee L; Browne N; Carroll TP; Meleady P; Henry M; McQuillan K; Murphy MP; Logan M; McCarthy C; McElvaney OJ; Reeves EP; McElvaney NG, Activation of complement component 3 is associated with airways disease and pulmonary emphysema in alpha-1 antitrypsin deficiency. Thorax 2020, 75 (4), 321–330. [PubMed: 31959730]
41. O'Brien ME; Murray G; Gogoi D; Yusuf A; McCarthy C; Wormald MR; Casey M; Gabillard-Lefort C; McElvaney NG; Reeves EP, A Review of Alpha-1 Antitrypsin Binding Partners for Immune Regulation and Potential Therapeutic Application. Int J Mol Sci 2022, 23 (5), 2441. [PubMed: 35269582]
42. Wu T; Dejanovic B; Gandham VD; Gogineni A; Edmonds R; Schauer S; Srinivasan K; Huntley MA; Wang Y; Wang TM; Hedehus M; Barck KH; Stark M; Ngu H; Foreman O; Meilandt WJ; Elstrott J; Chang MC; Hansen DV; Carano RAD; Sheng M; Hanson JE, Complement C3 Is Activated in Human AD Brain and Is Required for Neurodegeneration in Mouse Models of Amyloidosis and Tauopathy. Cell Rep 2019, 28 (8), 2111–2123 e6. [PubMed: 31433986]
43. Wetterling T; Tegtmeyer KF, Serum alpha 1-antitrypsin and alpha 2-macroglobulin in Alzheimer's and Binswanger's disease. Clin Investig 1994, 72 (3), 196–9.
44. Lisowska-Myjak B; Skarzynska E; Jakimiuk A, Links Between Vitamin D-Binding Protein, Alpha-1 Antitrypsin and Neutrophil Proteins in Meconium. Cell Physiol Biochem 2023, 57 (1), 15–22. [PubMed: 36751131]
45. Chen YH; Cheadle CE; Rice LV; Pfeffer PE; Dimeloe S; Gupta A; Bush A; Gooptu B; Hawrylowicz CM, The Induction of Alpha-1 Antitrypsin by Vitamin D in Human T Cells Is TGF-beta Dependent: A Proposed Anti-inflammatory Role in Airway Disease. Front Nutr 2021, 8, 667203. [PubMed: 34458299]
46. Khakzad H; Happonen L; Tran Van Nhieu G; Malmstrom J; Malmstrom L, In vivo Cross-Linking MS of the Complement System MAC Assembled on Live Gram-Positive Bacteria. Front Genet 2020, 11, 612475. [PubMed: 33488677]
47. Janssen BJ; Huizinga EG; Raaijmakers HC; Roos A; Daha MR; Nilsson-Ekdahl K; Nilsson B; Gros P, Structures of complement component C3 provide insights into the function and evolution of immunity. Nature 2005, 437 (7058), 505–11. [PubMed: 16177781]
48. Knopman DS; Amieva H; Petersen RC; Chetelat G; Holtzman DM; Hyman BT; Nixon RA; Jones DT, Alzheimer disease. Nat Rev Dis Primers 2021, 7 (1), 33. [PubMed: 33986301]
49. Husain MA; Laurent B; Plourde M, APOE and Alzheimer's Disease: From Lipid Transport to Physiopathology and Therapeutics. Front Neurosci 2021, 15, 630502. [PubMed: 33679311]
50. Chen Y; Strickland MR; Soranno A; Holtzman DM, Apolipoprotein E: Structural Insights and Links to Alzheimer Disease Pathogenesis. Neuron 2021, 109 (2), 205–221. [PubMed: 33176118]
51. Frieden C; Garai K, Structural differences between apoE3 and apoE4 may be useful in developing therapeutic agents for Alzheimer's disease. Proc Natl Acad Sci U S A 2012, 109 (23), 8913–8. [PubMed: 22615372]

52. Huang RY; Garai K; Frieden C; Gross ML, Hydrogen/deuterium exchange and electron-transfer dissociation mass spectrometry determine the interface and dynamics of apolipoprotein E oligomerization. Biochemistry 2011, 50 (43), 9273–82. [PubMed: 21899263]

53. Yamauchi Y; Deguchi N; Takagi C; Tanaka M; Dhanasekaran P; Nakano M; Handa T; Phillips MC; Lund-Katz S; Saito H, Role of the N- and C-terminal domains in binding of apolipoprotein E isoforms to heparan sulfate and dermatan sulfate: a surface plasmon resonance study. Biochemistry 2008, 47 (25), 6702–10. [PubMed: 18507396]

54. Snow AD; Cummings JA; Lake T, The Unifying Hypothesis of Alzheimer's Disease: Heparan Sulfate Proteoglycans/Glycosaminoglycans Are Key as First Hypothesized Over 30 Years Ago. Front Aging Neurosci 2021, 13, 710683. [PubMed: 34671250]

55. Zhang GL; Zhang X; Wang XM; Li JP, Towards understanding the roles of heparan sulfate proteoglycans in Alzheimer's disease. Biomed Res Int 2014, 2014, 516028. [PubMed: 25157361]

56. Katsouri L; Georgopoulos S, Lack of LDL receptor enhances amyloid deposition and decreases glial response in an Alzheimer's disease mouse model. PLoS One 2011, 6 (7), e21880. [PubMed: 21755005]

57. Dominguez C; Boelens R; Bonvin AM, HADDOCK: a protein-protein docking approach based on biochemical or biophysical information. J Am Chem Soc 2003, 125 (7), 1731–7. [PubMed: 12580598]

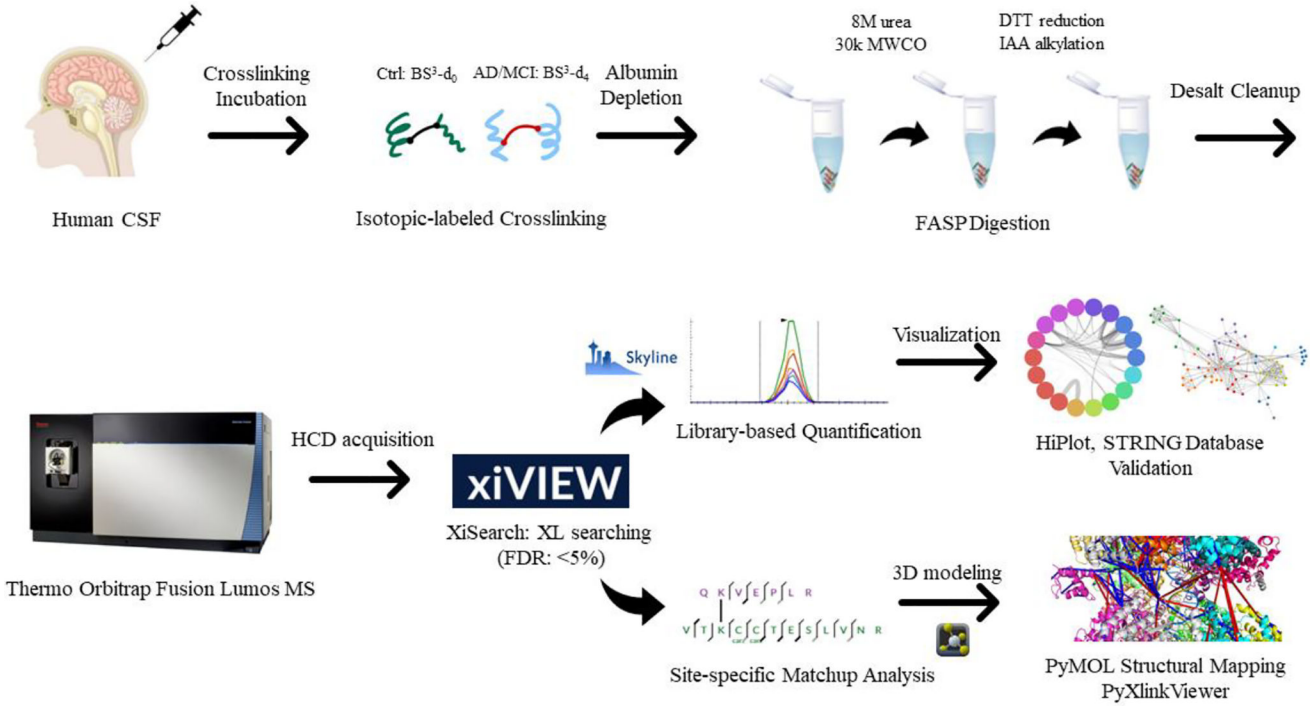

Figure 1.

The workflow of the quantitative crosslinking MS for analysis of the protein structural changes and protein-protein network conformational changes in human CSF samples.

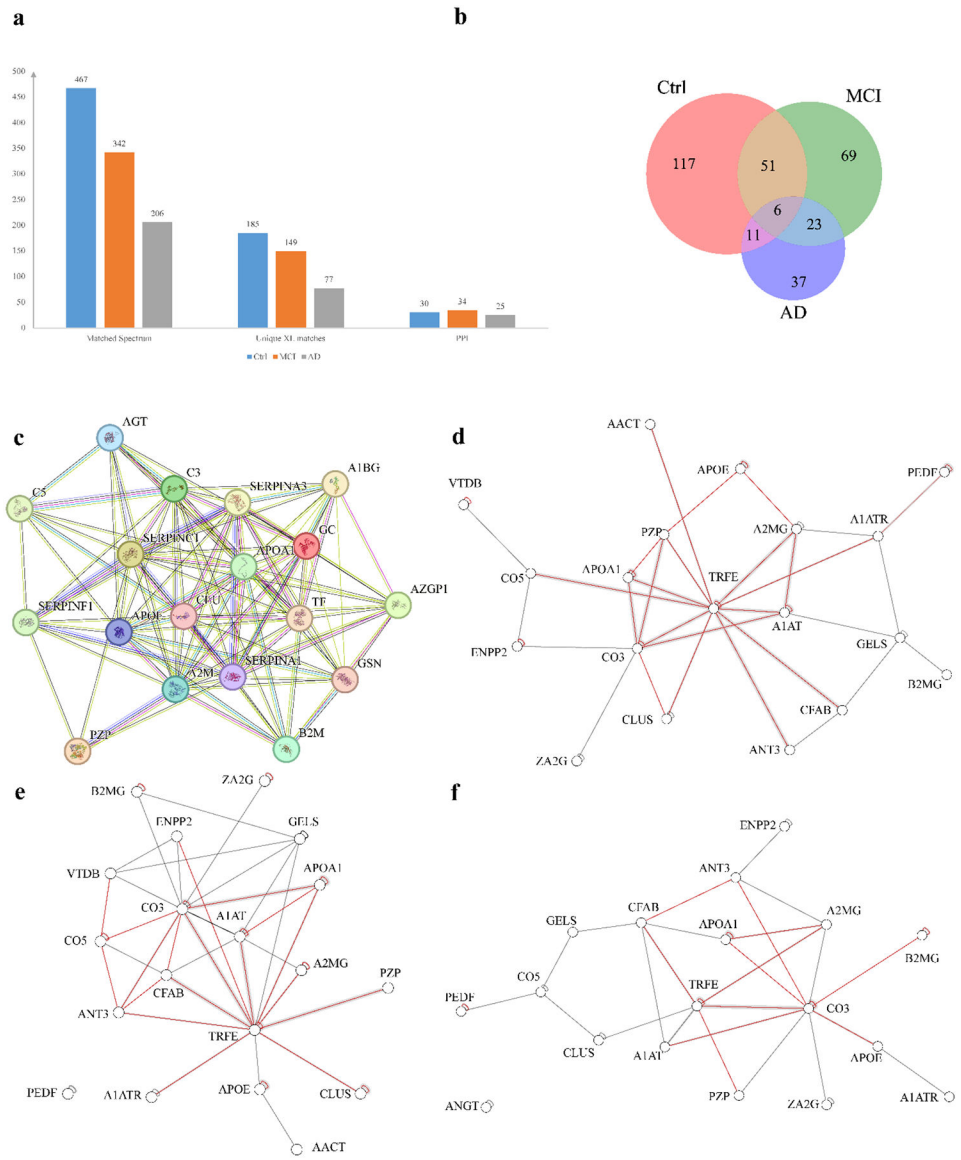

Figure 2. The experimental outcome of the crosslinking MS.

(a) The comparison of the number of matched spectra, unique crosslinking matches and PPI for Ctrl, MCI and AD sample groups under XiSearch searching. (b) Venn diagram for the specific crosslinking matches in each condition. (c) The STRING database interaction diagram of the high-confident candidates. (d) Visualization mapping of the pairwise unique crosslinking matches via xiView in Ctrl group and (e) MCI and (f) AD group. The crosslinking between the proteins with more than 3 unique site-specific matched pairs are highlighted.

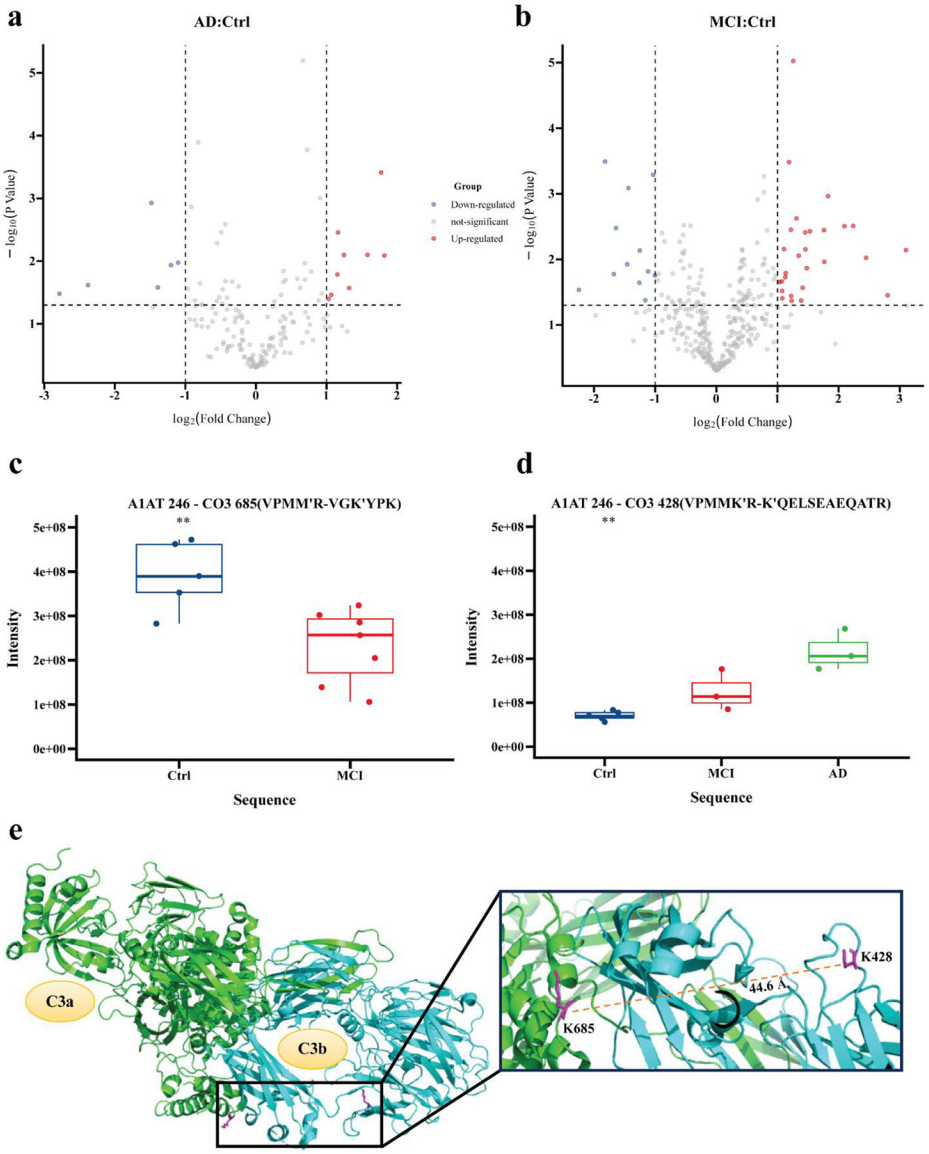

Figure 3. Quantitative crosslink matchups derived from Skyline.

(a) the volcano plot of the quantitative crosslinking pairs from Skyline in the AD:Ctrl set and (b) in the MCI:Ctrl set. In the case study of interlink between CO3 and A1AT, the abundance changes between (c) A1AT K246 and CO3 K685 and (d) A1AT K246 and CO3 K428 are provided. (e) The crystal structure of C3 (PDB: 2A73) is labeled with K685 and K428 in purple.

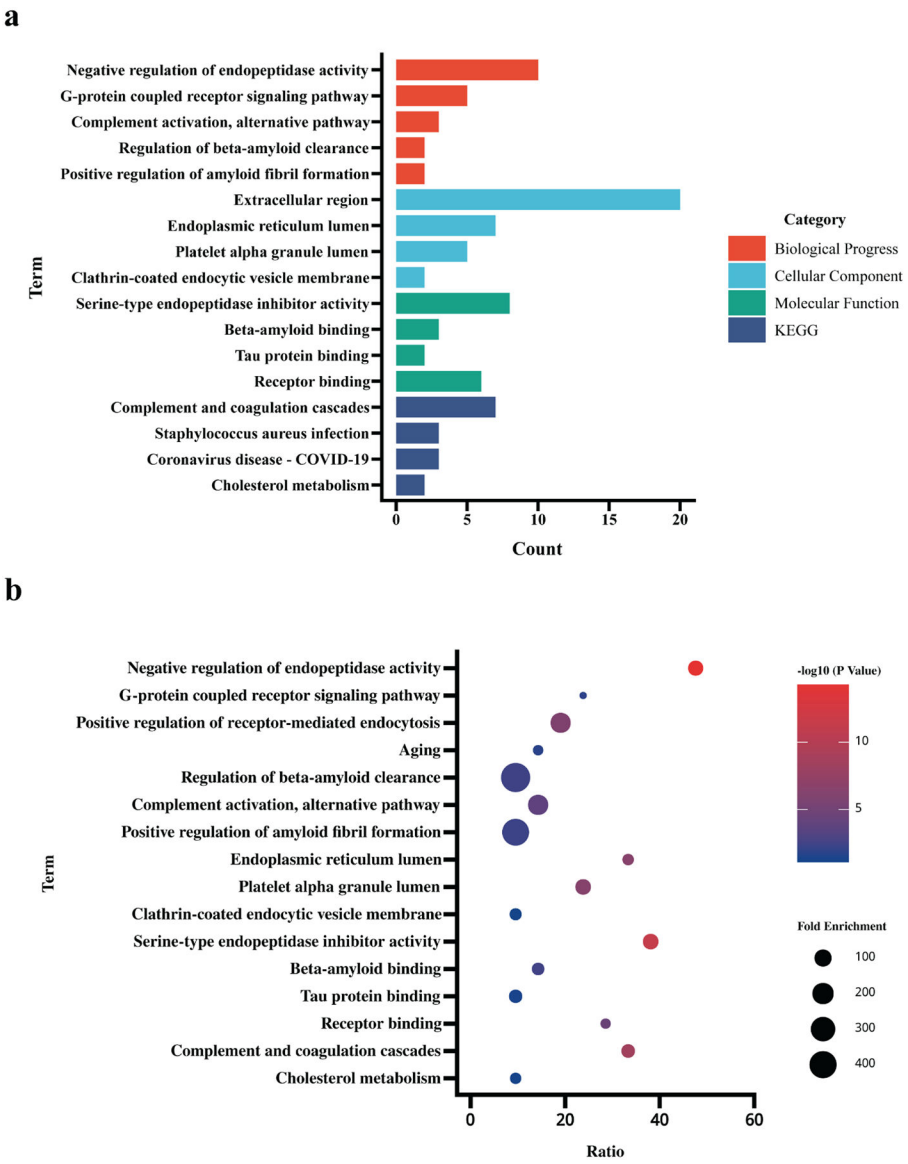

Figure 4. GO enrichment and KEGG pathway analysis based on identified crosslinked biomarkers.

(a) Bar chart of GO enrichment and KEGG pathway analysis of the significantly modified proteins during AD development. (b) Bubble chart of AD-related terms associated with crosslink represented structural changes.

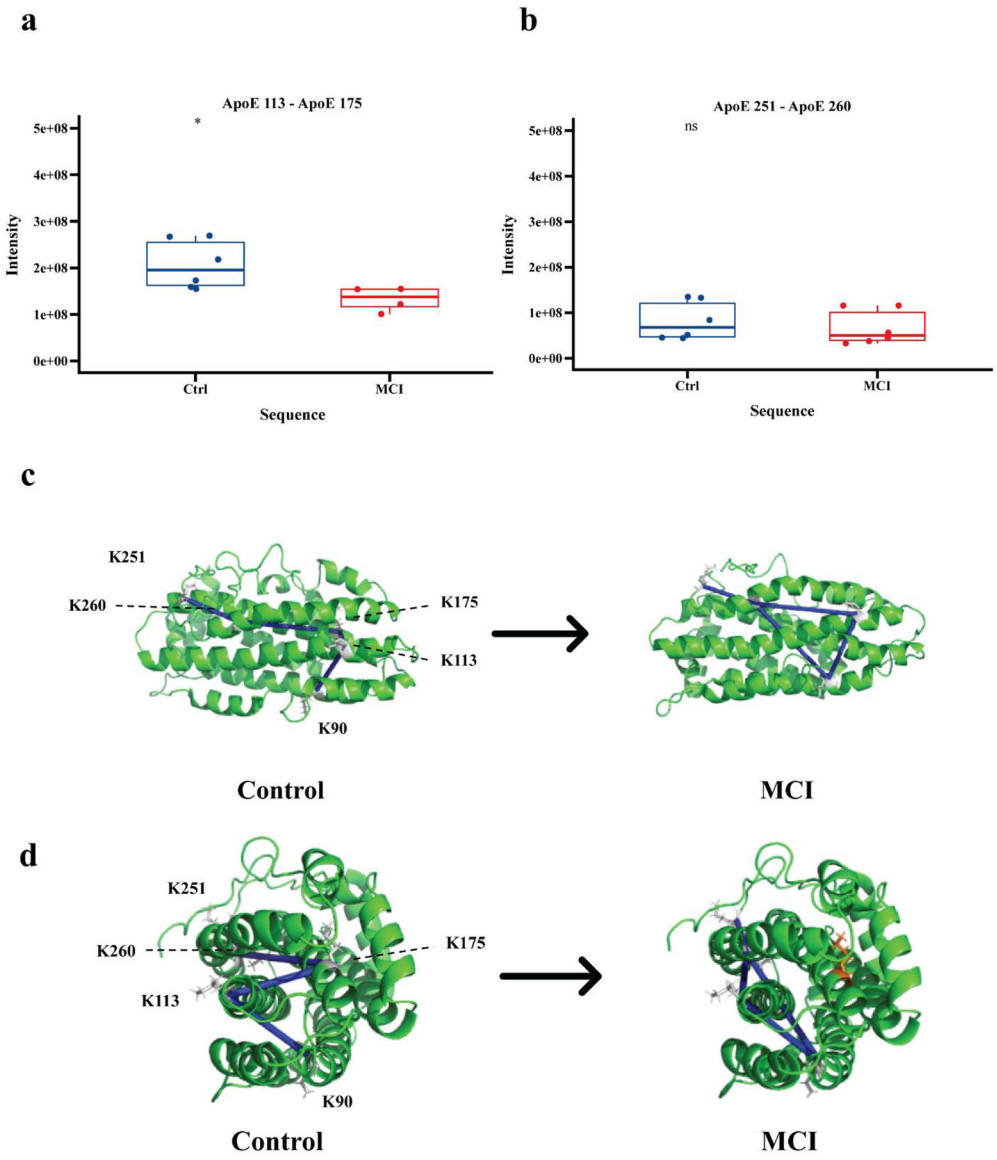

Figure 5. Intralinks within ApoE reveals a conformational change during MCI progression.
Quantitative comparison of the abundance between healthy control and MCI sample in (a) APOE K251-K260 and (b) K113-K175. The overview (c) and sideview (d) of the demonstration of crosslink within PyMOL model (PDB: 2L7B), as K175 highlighted in orange.